LLR Shaping Technique for Achievement of High NGMI for SD-FEC Scheme in 128-Gbaud PAM4 10-km Transmission with Advanced MLSE

Shuto Yamamoto[1], Hiroki Taniguchi[1], Akira Masuda[1], Masanori Nakamura[1], Yoshiaki Kisaka[1]

[1] NTT Network Innovation Laboratories, NTT Corporation, shuto.yamamoto@ntt.com

Abstract *We propose a simple method to calculate LLR for IM-DD system with MLSE and SD-FEC. We show that an advanced MLSE with the simple calculation method which shapes the LLR distribution makes NGMI higher for 128-Gbaud PAM4 signal in a severe bandwidth limitation.*

Introduction

The amount of data-centre traffic is recently increasing due to the massive use of cloud services handling rich contents. Ethernet is deployed and applied to intra data centre networks to economically support a huge number of connection ports. In IEEE802.3, Ethernet has been already completed standardization up to 400GbE at 100-Gbps per channel with O-band and intensity-modulation and direct-detection (IM-DD) schemes [1]. The higher modulation rate leads to bandwidth limitation (BWL) by transceiver components and sensitivity degradation due to decreasing the number of photons per symbol. For BWL, several studies about solving severe inter-symbol interference (ISI) in IM-DD systems are reported [2-10], and maximum likelihood sequence estimation (MLSE) has attracted much attention [11-13]. For sensitivity degradation, an application of soft decision (SD) forward error correction (FEC) is discussed in IEEE802.3 [14, 15]. SD-FEC is performed based on logarithm likelihood ratio (LLR), which is conventionally calculated by soft-output Viterbi algorithm (SOVA) in MLSE scheme and the calculation is very complicated [16].

In this paper, we propose a simple method of LLR calculation for IM-DD system with an advanced MLSE and SD-FEC in which LLR shaping technique is applied and the complexity is less than that in SOVA. We demonstrate O-band 128-Gbaud PAM4 10-km transmission with 10-dB bandwidth of 40 GHz and the simple LLR calculation method achieves the higher performance in normalized generalized mutual information (NGMI) which corresponds to performance index in SD-FEC system.

Simple LLR calculation and LLR shaping

We propose a simple method of LLR calculation. At first, a temporal LLR is calculated from the minimum value of path metric for each bit composing PAM4 symbol in Viterbi algorithm (VA) as shown below [17].

$$LLR_{temp} = \left(\min_{i \in U_0} l_i - \min_{i \in U_1} l_i\right)/(2\sigma^2), \quad (1)$$

where l_i is the i-th path metric in VA. U_j is a set of indexes corresponding to bit $j \in \{0,1\}$. σ is a standard deviation of the noise distribution in a transmission channel. This method is called Method A in this paper. Method A is very simple but a gain from a trace back is not obtained in this method. The trace back is corresponding to backward sequence estimation in VA and enhances the accuracy of bit decision. Therefore, Method A may not always achieve high performance.

Next, the temporal LLR is updated according to the result from the trace back. When the bit decision based on the trace back indicates bit 0 or 1, the temporal LLR is updated based on Eq. (2). a is a shaping parameter and $b_{\pm}$ is a shift parameter. b_- is corresponding to the case in which the bit decision based on the trace back is bit 0 while b_+ is corresponding to the case with bit 1. In this equation, a is 0 or positive. b_- and b_+ are negative and positive values, respectively. Here, $b_+ = -b_- = b$ for simplicity. This method is called Method B in this paper. As shown in Eq. (2), Method B includes an effect of the trace back. Equation (2) is corresponding to shaping the distribution of LLR_{temp} based on the decision obtained by the trace back in VA. Therefore, it is expected for Method B to realize the higher NGMI than that based on Method A.

Figures 1 (a) and (b) show the required numbers of path-metric data for calculation of LLR in Methods A, B, and SOVA. M is the number of PAM levels. d is the memory length of

$$LLR = \frac{1}{2\sigma^2}\left(\frac{2\sigma^2 LLR_{temp} - b_{\pm}}{1+a} + b_{\pm}\right) = \frac{\min_{i \in U_0} l_i - \min_{i \in U_1} l_i + ab_{\pm}}{2\sigma^2(1+a)} \quad (2)$$

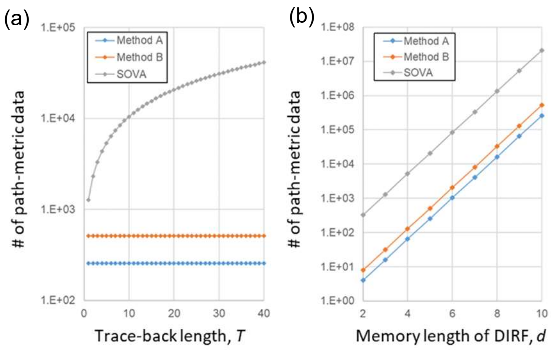

Fig. 1: (a) Trace-back length dependency and (b) memory length dependency of the number of path-metric data for LLR calculation. In (a), $M = 4$, $d = 5$. In (b), $M = 4$, $T = 20$.

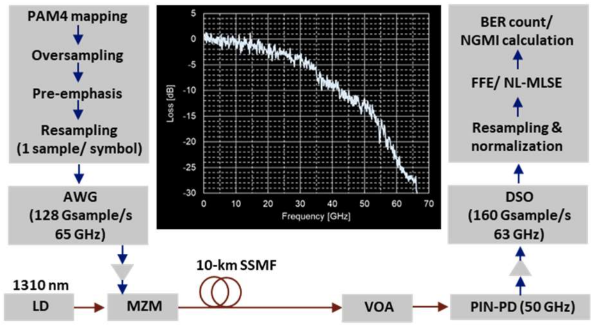

Fig. 2: Experimental configuration and frequency response of transmission system, in which 10-dB bandwidth is about 40 GHz.

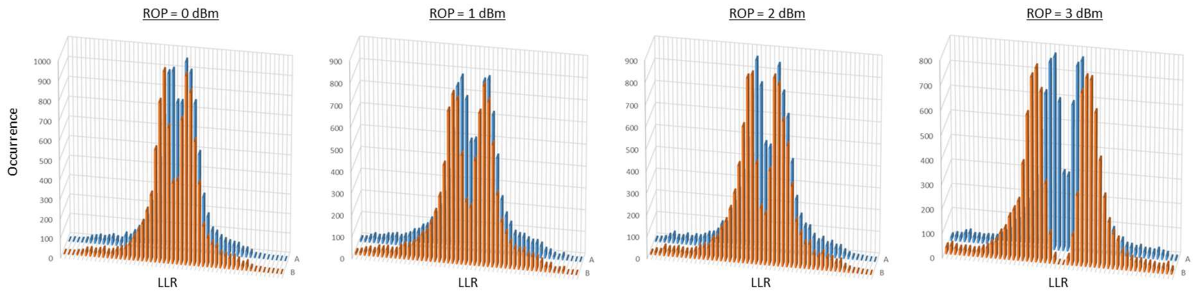

Fig. 3: Histograms of LLR distribution obtained from LLR calculation based on Methods A and B in ROPs of 0 dBm, 1 dBm, 2 dBm, and 3 dBm. Results from Methods A and B are shown as blue and red bars, respectively. The blue and red bars correspond to the distributions before LLR shaping and after LLR shaping, respectively. The LLR shaping makes the distribution shaper. For each ROP, $a = 0.005$, $b = 0.04$.

a desired impulse response filter (DIRF) in MLSE. T is a trace-back length in VA. In Fig. 1 (a), $M = 4$ and $d = 5$. In Fig. 1 (b), $T = 20$ and $M = 4$. For example, Fig. 1 (a) shows that the required numbers of path-metric data in Methods A and B are 2.4% and 4.9% of that in SOVA at $T = 10$, $M = 4$, $d = 5$, respectively. Figure 1 (b) shows that the required numbers of path-metric data in Methods A and B are 1.2% and 2.5% of that in SOVA at $T = 20$, $M = 4$, respectively. These results mean that Methods A and B are much simpler than SOVA.

Experimental configuration

We investigate demodulation performances of Methods A and B through 128-Gbaud PAM4 10-km O-band transmission using NL-MLSE [18] as an advanced MLSE. We measure bit error ratio (BER) and NGMI, which are corresponding to the performance indexes in hard-decision FEC (HD-FEC) and SD-FEC systems, respectively. The experimental configuration is shown in Fig. 2. Electrical signal sequence is generated by a 128-Gsample/s arbitrary waveform generator (AWG) in which pseudo-random binary sequence (PRBS) order is 15. The electrical signal is converted into optical signal at 1310 nm by a Mach-Zehnder modulator (MZM). The optical signal is transmitted through 10-km standard single-mode fibre (SSMF) without optical amplifiers and received with a PIN photodiode (PD), in which the chromatic dispersion (CD) is -8.0 ps/nm at 1310 nm. The received optical power (ROP) is adjusted by a variable optical attenuator (VOA). The received signal is converted into a digital signal sequence by a 160-Gsample/s digital storage oscilloscope (DSO) and demodulated by the conventional feed forward equalizer (FFE) or NL-MLSE with the trace-back length of 20. The finite impulse response (FIR) filter has 45 T/2-spaced taps. Adaptive low-pass filter (ALPF) and DIRF have T-spaced taps and the memory length is 5. These filters are updated by recursive least square (RLS) algorithm. The order of Volterra series expansion in DIRF is 3. The filter taps and

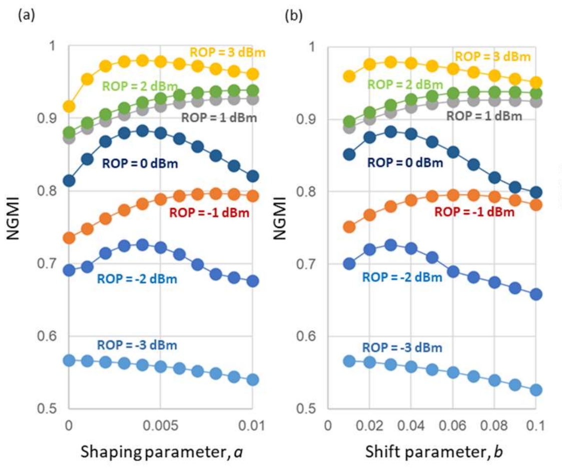

Fig. 4: (a) Shaping parameter dependency and (b) shift parameter dependency of NGMI in Method B for several ROPs. In (a), *b* = 0.04. In (b), *a* = 0.005. For several ROPs, the better values of *a* and *b* are around 0.005 and 0.04, respectively.

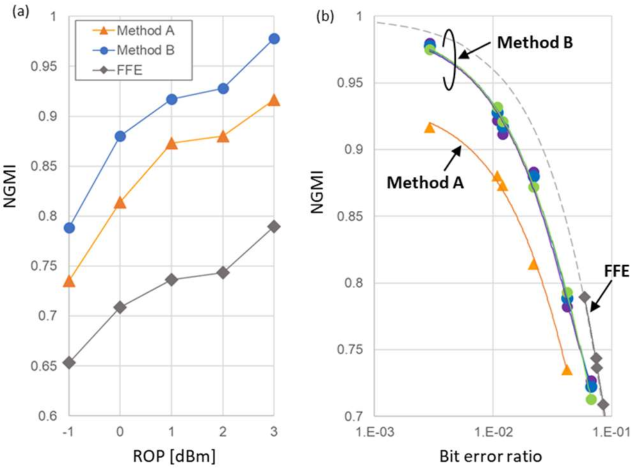

Fig. 5: (a) Relationship between ROP and NGMI, where *a* = 0.005 and *b* = 0.04 for Method B. (b) Relationship between BER and NGMI, where *b* = 0.04 for Method B. Purple, blue, and green plots correspond to *a* = 0.004, 0.005, and 0.006, respectively.

Volterra kernels are pre-trained by the first 1000 symbols to ensure the correct adaptation of the filters. As shown in Fig. 2, 10-dB bandwidth of the transmission system is about 40 GHz.

Experimental Results

Figure 3 shows histograms of LLR distribution in Methods A and B. The blue and red bars are corresponding to the distributions in Methods A and B, respectively. As shown in Fig. 3, Method B realizes the sharper LLR distribution than that in Method A. In Method B, the information obtained from trance back sharpens the LLR distribution of Method A. The shaped LLR distribution achieves the higher NGMI.

Figures 4 (a) and (b) show the relationship between parameter a and NGMI, and the relationship between parameter b and NGMI, respectively. NGMI is calculated based on bit-wise LLR [19]. The parameters are set on $b = 0.04$ and $a = 0.005$ in Figs. 4 (a) and (b), respectively. The better value of a is around 0.005 while the better value of b is around 0.04 for several ROPs.

Figure 5 (a) shows the relationship between ROP and NGMI for the conventional FFE scheme and NL-MLSE scheme with Method A or B, in which $a = 0.005$ and $b = 0.04$ for Method B. As shown in this figure, Methods A and B achieve the NGMI higher than that in the FFE scheme for each ROP.

Figure 5 (b) shows the relationship between BER and NGMI. For Method B, a is 0.004, 0.005, or 0.006, and b is 0.04. The FFE scheme is not able to achieve 0.8 of NGMI. Methods A and B achieve 0.92 and 0.98 of NGMI, respectively. This means that the LLR shaping improves NGMI by 7%. The dashed line in Fig. 6 is corresponding to the theoretical curve in additive white Gaussian noise (AWGN) channel and SOVA realizes the almost same performance with the theoretical curve. Therefore, it is assumed that SOVA achieve 0.99 of NGMI. This means that NGMI achieved by Method B is very close to that by SOVA.

Conclusion

We proposed a simple LLR calculation in IM-DD system with MLSE and SD-FEC. The calculation method shaped the LLR distribution based on a trace back in VA and the shaped LLR distribution achieved the higher NGMI. The calculation method required the complexity much less than that in SOVA. We investigated an advanced MLSE scheme with the proposed calculation method through a 128-Gbaud PAM4 10-km O-band transmission experiment and we showed that the proposed method achieved the higher performance not only in BER but also in NGMI than that of a conventional linear equalization scheme. As a result, it is indicated that MLSE schemes are applicable to high-baudrate system with SD-FEC utilizing uncomplicated digital signal processing.

References

[1] IEEE 802.3cu-2021 - IEEE Standard for Ethernet - Amendment 11: Physical Layers and Management

Parameters for 100 Gb/s and 400 Gb/s Operation over Single-Mode Fiber at 100 Gb/s per Wavelength.

[2] L. Mineli, et al., “Net 100 Gb/s/l VCSEL+MMF nonlinear digital pre-distortion using convolutional neural networks,” in *Proceedings OFC*, Tu3I.4 (2023)

[3] G. Boecherer, et al., “Spiking neural network linear equalization: experimental demonstration of 2km 100Gb/s IM/DD PAM4 optical transmission,” in *Proceedings OFC*, W4E.1 (2023)

[4] D. Che, et al., “Comparison between PAM and DMT in a 200-Gb/s IM-DD system considering the interaction between bandwidth limit and peak power constraint at transmitter,” *in Proceedings OFC*, W4E.4 (2023)

[5] J. Cho, et al., “Volterra equalization to compensate for transceiver nonlinearity: performance and pitfalls,” in *Proceedings OFC*, W2A.36 (2022)

[6] D. Plabst, et al., “Experiments on bipolar transmission with direct detection,” in *Proceedings ECOC*, We2D.5 (2022)

[7] M. S. B. Hossain, et al., “Experimental comparison of PAM-8 probabilistic shaping with different Gaussian orders at 200 Gb/s net rate in IM/DD system with O-band TOSA,” in *Proceedings ECOC*, WeD.3 (2022)

[8] X. Chen, et al., “Single-wavelength and single-photodiode 700 Gb/s entropy-loaded PS-256-QAM and 200-Gbaud PS-PAM-16 transmission over 10-km SMF,” in *Proceedings ECOC*, Th3A-2 (2020)

[9] Q. Hu, et al., “120 Gbaud IM/DD PAM-4 transmission over 1.5 km SMF using a single CMOS DAC with < 20 GHz analog bandwidth,” in *Proceedings ECOC*, Tu1E-5 (2020)

[10] X. Li, et al., “102 Gbaud PAM-4 transmission over 2 km using a pulse shaping filter with asymmetric ISI and Tomlinson-Harashima precoding,” in *Proceedings OFC*, T3I.1 (2020)

[11] N. Stojanovic, et al., “Performance and DSP complexity evaluation of a 122-Gbit/s PAM-4 transceiver employing a 25-GHz TOSA and ROSA,” in *Proceedings ECOC*, Mo.4.5.5 (2015)

[12] N. Eiselt, et al., “Experimental demonstration of 112-Gbit/s PAM-4 over up to 80 km SSMF at 1550 nm for inter0DCI applications,” in *Proceedings ECOC*, M.2.D.1 (2016)

[13] S. Yamamoto, et al., “Spectral-shaping technique based on nonlinear-coded-modulation for short-reach optical transmission,” *Journal of Lightwave Technology*, vol. 38, no. 2, pp.466-474 (2020)

[14] https://www.ieee802.org/3/df/public/22_02/lu_3df_01b_220215.pdf

[15] https://www.ieee802.org/3/df/public/22_02/wang_3df_01_220215.pdf

[16] J. Hagenauer, et al., “A Viterbi algorithm with soft-decision outputs and its applications,” in *Proceedings IEEE Global Telecommunications Conference and Exhibition*, pp.1680-1686 (1989)

[17] S. Yamamoto, et al., “Evaluation of NGMI in 128-Gbaud PAM4 O-band 10-km transmission using MLSE based on nonlinear channel estimation and decision feedback,” in *Proceedings ECOC*, We5.26 (2022)

[18] H. Taniguchi, et al., “Advanced O-band transmission using maximum likelihood sequence estimation,” in *Proceedings ECOC*, We2D.1 (2022)

[19] A. Alvarado, et al., “Replacing the soft-decision FEC limit paradigm in the design of optical communication systems,” *Journal of Lightwave Technology*, vol. 33, no. 20, pp.4338-4352 (2015)